Supplementary Appendix

Supplement to: Kissler SM, Fauver JR, Mack C, et al. Viral dynamics of SARS-CoV-2 variants in vaccinated and unvaccinated persons. N Engl J Med. DOI: 10.1056/NEJMc2102507

This appendix has been provided by the authors to give readers additional information about the work.

Contents.

Supplementary Methods.

Study design. The data reported here represent a convenience sample including team staff, players, arena staff, and other vendors (e.g., transportation, facilities maintenance, and food preparation) affiliated with the National Basketball Association (NBA). The study period ran between November 28th, 2020, and August 11th, 2021. Clinical samples were obtained by combined swabs of the anterior nares and oropharynx administered by a trained provider. Viral concentration was measured using the cycle threshold (Ct) according to the Roche cobas target 1 assay. Ct values were converted to viral genome equivalents using a standard curve (**"**Converting Ct values to viral genome equivalents").

Study oversight. In accordance with the guidelines of the Yale Human Investigations Committee, this work with de-identified samples was approved for research not involving human subjects by the Yale Institutional Review Board (HIC protocol # 2000028599). This project was designated exempt by the Harvard Institutional Review Board (IRB20-1407).

Study participants. Out of an initial pool of 872 participants who tested positive for SARS-CoV-2 infection during the study period, 173 individuals (90% male) had clinically confirmed novel infections that met our inclusion criteria: at least three positive PCR tests (Ct < 40), at least one negative PCR test (Ct = 40), and at least one test with Ct < 32 with the first positive test (Ct <40) occurring before August 1st to ensure full sampling of the trajectory before the end of the study period (**Table S1**). A total of 19,941 samples were available for this cohort, averaging 548 samples per week. Of the individuals who met the inclusion criteria, 36 were infected with alpha (B.1.1.7) and 36 with delta (B.1.617.2, AY.1, AY.2, AY.3, or AY.3.1), as confirmed by sequencing. An additional 28 individuals were infected with other variants of interest/variants of concern. There were 37 individuals with vaccine breakthrough infections, defined as infections for which the first positive test occurred at least two weeks after receipt of the final dose. Of these, 23 received the Pfizer-BioNTech vaccine, 8 received the Johnson & Johnson/Janssen vaccine, and 3 received the Moderna vaccine. The vaccine manufacturer was not reported for the remaining 3 individuals.

Study outcomes. We quantified the viral proliferation duration (time from first possible detection to peak viral concentration) the viral clearance duration (time from peak viral concentration to clearance of acute infection), the duration of acute infection (proliferation duration plus clearance

duration), and the peak viral concentration for each person. We also quantified the population mean values of these quantities separately for individuals infected with alpha (n = 36), delta (n = 36), and non-VOI/VOCs (n = 41), as well as for vaccinated (n = 37) and unvaccinated (n = 136) individuals.

Genome sequencing and lineage assignments. RNA was extracted and confirmed as SARS-CoV-2 positive by RT-qPCR with the Thermo Fisher TaqPath SARS-CoV-2 assay.[1] Next Generation Sequencing with the Illumina COVIDSeq ARTIC primer set[2] was used for viral amplification. Library preparation was performed using the amplicon-based Illumina COVIDseq Test v03[3] and sequenced 2x74 on Illumina NextSeq 550 following the protocol as described in Illumina's documentation.[4] The resulting FASTQs were processed and analyzed on Illumina BaseSpace Labs using the Illumina DRAGEN COVID Lineage Application;[5] versions included are 3.5.0, 3.5.1, 3.5.2, and 3.5.3. The DRAGEN COVID Lineage pipeline was run with default parameters recommended by Illumina. Samples were considered SARS-COV-2 positive if at least 5 viral amplicon targets were detected at 20x coverage. Each SARS-COV-2 positive sample underwent lineage assignment and phylogenetics analysis using the most updated version of Pangolin[6] and NextClade,[7] respectively.

Converting Ct values to viral genome equivalents. To convert Ct values to viral genome equivalents, we first converted the Roche cobas target 1 Ct values to equivalent Ct values on a multiplexed version of the RT-qPCR assay from the US Centers for Disease Control and Prevention.[8] We did this following our previously described methods.[9] Briefly, we adjusted the Ct values using the best-fit linear regression between previously collected Roche cobas target 1 Ct values and CDC multiplex Ct values using the following regression equation:

$$y_i = \beta_0 + \beta_1 x_i + \epsilon_i \quad \text{(S1)}$$

Here, y_i denotes the i^{th} Ct value from the CDC multiplex assay, x_i denotes the i^{th} Ct value from the Roche cobas target 1 test, and ε_i is an error term with mean 0 and constant variance across all samples. The coefficient values are $\beta_0 = -6.25$ and $\beta_1 = 1.34$.

Ct values were fitted to a standard curve to convert Ct value data to RNA copies. Synthetic T7 RNA transcripts corresponding to a 1,363 b.p. segment of the SARS-CoV-2 nucleocapsid gene

were serially diluted from 10^6-10^0 RNA copies/µl in duplicate to generate a standard curve[10] (**Table S3**). The average Ct value for each dilution was used to calculate the slope (-3.60971) and intercept (40.93733) of the linear regression of Ct on $\log_{10}$ transformed standard RNA concentration, and Ct values from subsequent RT-qPCR runs were converted to RNA copies using the following equation:

$$\log_{10}([\mathrm{RNA}]) = (Ct - 40.93733)/(-3.60971) + \log_{10}(250) \quad \text{(S2)}$$

Here, [RNA] represents the RNA copies /ml. The $\log_{10}(250)$ term accounts for the extraction (300 µl) and elution (75 µl) volumes associated with processing the clinical samples as well as the 1,000 µl/ml unit conversion.

Statistical analysis. Following previously described methods,[9] we used a Bayesian hierarchical model to estimate the proliferation duration, clearance duration, and peak viral concentration for each person and for the sub-populations of interest. The model describes the $\log_{10}$ viral concentration during an acute infection using a continuous piecewise-linear curve with control points that specify the time of acute infection onset, the time and magnitude of peak viral concentration, and the time of acute infection clearance. The assumption of piecewise linearity is equivalent to assuming exponential viral growth during the proliferation period followed by exponential viral decay during the clearance period. The control points were inferred using the Hamiltonian Monte Carlo algorithm as implemented in Stan (version 2.24).[11] We used priors informed by a previous analysis[9] for the main analysis and conducted a sensitivity analysis using vague priors as well as a strongly biased set of priors to assess robustness to the choice of prior. Full details are given in the **Supplementary methods.** Data and code are available online.[12]

Model fitting.

For the statistical analysis, we removed any sequences of 3 or more consecutive negative tests (Ct = 40) to avoid overfitting to these trivial values. Following our previously described methods,[9] we assumed that the viral concentration trajectories consisted of a proliferation phase, with exponential growth in viral RNA concentration, followed by a clearance phase characterized by exponential decay in viral RNA concentration.[13] Since Ct values are roughly proportional to the negative logarithm of viral concentration[14], this corresponds to a linear decrease in Ct followed by a linear increase. We therefore constructed a piecewise-linear regression model to estimate the

peak Ct value, the time from infection onset to peak (*i.e.* the duration of the proliferation stage), and the time from peak to infection resolution (*i.e.* the duration of the clearance stage). The trajectory may be represented by the equation

$$E[Ct(t)] = \begin{cases} \text{l.o.d.} & t \leq t_o \\ \text{l.o.d.} - \frac{\delta}{t_p - t_o}(t - t_o) & t_o < t \leq t_p \\ \text{l.o.d.} - \delta + \frac{\delta}{t_r - t_p}(t - t_p) & t_p < t \leq t_r \\ \text{l.o.d.} & t > t_r \end{cases} \quad \text{(S3)}$$

Here, E[*Ct(t)*] represents the expected value of the Ct at time *t,* "l.o.d" represents the RT-qPCR limit of detection, δ is the absolute difference in Ct between the limit of detection and the peak (lowest) Ct, and t_o, t_p, and t_r are the onset, peak, and recovery times, respectively.

Before fitting, we re-parametrized the model using the following definitions:

- $\Delta Ct(t)$ = l.o.d. – *Ct(t)* is the difference between the limit of detection and the observed Ct value at time *t.*
- $\omega_p = t_p - t_o$ is the duration of the proliferation stage.
- $\omega_r = t_r - t_p$ is the duration of the clearance stage.

We constrained $0.25 \leq \omega_p \leq 14$ days and $2 \leq \omega_r \leq 30$ days to prevent inferring unrealistically small or large values for these parameters for trajectories that were missing data prior to the peak and after the peak, respectively. We also constrained $0 \leq \delta \leq 40$ as Ct values can only take values between 0 and the limit of detection (40).

We next assumed that the observed $\Delta Ct(t)$ could be described the following mixture model:

$$\Delta Ct(t) \sim \lambda \, \text{Normal}(E[\Delta Ct(t)], \sigma(t)) + (1 - \lambda) \, \text{Exponential}(\log(10)) \Big]_0^{\text{l.o.d}} \quad \text{(S4)}$$

where E[$\Delta Ct(t)$] = l.o.d. - E[*Ct(t)*] and λ is the sensitivity of the q-PCR test, which we fixed at 0.99. The bracket term on the right-hand side of the equation denotes that the distribution was truncated to ensure Ct values between 0 and the limit of detection. This model captures the scenario where

most observed Ct values are normally distributed around the expected trajectory with standard deviation $\sigma(t)$, yet there is a small (1%) probability of an exponentially distributed false negative near the limit of detection. The log(10) rate of the exponential distribution was chosen so that 90% of the mass of the distribution sat below 1 Ct unit and 99% of the distribution sat below 2 Ct units, ensuring that the distribution captures values distributed at or near the limit of detection. We did not estimate values for λ or the exponential rate because they were not of interest in this study; we simply needed to include them to account for some small probability mass that persisted near the limit of detection to allow for the possibility of false negatives.

We used a hierarchical structure to describe the distributions of ω_p, ω_r, and δ for each person based on their respective population means $\mu_{\omega p}$, $\mu_{\omega r}$, and μ_δ and population standard deviations $\sigma_{\omega p}$, $\sigma_{\omega r}$, and σ_δ such that

$$\begin{aligned}\omega_p &\sim \text{Normal}(\mu_{\omega p}, \sigma_{\omega p})\\ \omega_r &\sim \text{Normal}(\mu_{\omega r}, \sigma_{\omega r})\\ \delta &\sim \text{Normal}(\mu_\delta, \sigma_\delta)\end{aligned} \tag{S5}$$

We inferred population means ($\mu_\cdot$) separately for individuals infected with alpha, delta, and non-VOI/VOCs, as well as for unvaccinated and vaccinated individuals in a separate analysis. We used a Hamiltonian Monte Carlo fitting procedure implemented in Stan (version 2.24)[11] and R (version 3.6.2)[15] to estimate the individual-level parameters ω_p, ω_r, δ, and t_p as well as the population-level parameters σ^*, $\mu_{\omega p}$, $\mu_{\omega r}$, μ_δ, $\sigma_{\omega p}$, $\sigma_{\omega r}$, and σ_δ. We used the following priors:

Hyperparameters:

$$\sigma^* \sim \text{Cauchy}(0, 5)\ [0, \infty] \tag{S6}$$

$$\begin{aligned}\mu_{\omega p} &\sim \text{Normal}(2.7, 14/6)\ [0.25, 14]\\ \mu_{\omega r} &\sim \text{Normal}(7.4, 30/6)\ [2, 30]\\ \mu_\delta &\sim \text{Normal}(20, 40/6)\ [0, 40].\end{aligned} \tag{S7}$$

$$\begin{aligned}\sigma_{\omega p} &\sim \text{Cauchy}(0, 14/\tan(\pi(0.95\text{-}0.5)))\ [0, \infty]\\ \sigma_{\omega r} &\sim \text{Cauchy}(0, 30/\tan(\pi(0.95\text{-}0.5)))\ [0, \infty]\end{aligned} \tag{S8}$$

$\sigma_\delta \sim$ Cauchy(0, 40/tan(π(0.95-0.5))) [0, ∞]

Individual-level parameters:

$\omega_p \sim$ Normal($\mu_{\omega p}$, $\sigma_{\omega p}$) [0.25,14]

$\omega_r \sim$ Normal($\mu_{\omega r}$, $\sigma_{\omega r}$) [2,30] (S9)

$\delta \sim$ Normal(μ_δ, σ_δ) [0,40]

$t_p \sim$ Normal(0, 2)

The values in square brackets denote truncation bounds for the distributions. We chose a vague half-Cauchy prior with scale 5 for the observation variance σ^*. The priors for the population mean values ($\mu_\cdot$) are normally distributed priors spanning the range of allowable values for that parameter; this prior is vague but expresses a mild preference for values near the posterior estimates obtained from a previous analysis.[16] The priors for the population standard deviations ($\sigma_\cdot$) are half Cauchy-distributed with scale chosen so that 90% of the distribution sits below the maximum value for that parameter; this prior is vague but expresses a mild preference for standard deviations close to 0.

We ran four MCMC chains for 2,000 iterations each with a target average proposal acceptance probability of 0.8. The first half of each chain was discarded as the warm-up. The Gelman R-hat statistic was less than 1.1 for all parameters. This indicates good overall mixing of the chains. There were no divergent iterations, indicating good exploration of the parameter space. The posterior distributions for μ_δ, $\mu_{\omega p}$, and $\mu_{\omega r}$, were estimated separately for individuals infected with alpha, delta, and non-VOI/VOCs as well as for vaccinated and unvaccinated individuals. These are depicted in **Figures S1–S2**. Draws from the individual posterior viral trajectory distributions are depicted in **Figures S3-S11.** We also assessed posterior mean trajectories for vaccinated *vs.* unvaccinated individuals while restricting to delta infections (**Figure S12**) and for vaccinated individuals who received the Pfizer-BioNTech *vs.* the Johnson & Johnson/Janssen vaccine (**Figure S13**). The mean posterior viral trajectories for each person are depicted in **Figure S14**.

Assessing sensitivity to different priors.

To ensure that our findings were not overly influenced by the prior distributions, we re-fit the model using two different sets of priors. The first "vague" set used posterior population means for $\mu_{\omega p}$,

$\mu_{\omega r}$, and μ_{δ} chosen to lie near the center of the allowable range for those parameters. These priors were defined by

$$\begin{aligned} \mu_{\omega p} &\sim \text{Normal}(14/2, 14/6)\ [0.25, 14] \\ \mu_{\omega r} &\sim \text{Normal}(30/2, 30/6)\ [2, 30] \\ \mu_{\delta} &\sim \text{Normal}(40/2, 40/6)\ [0, 40] \end{aligned} \tag{S10}$$

The second set used unrealistically low prior means for $\mu_{\omega p}$, $\mu_{\omega r}$, and μ_{δ} to check model robustness to highly biased prior distributions. These priors were defined by

$$\begin{aligned} \mu_{\omega p} &\sim \text{Normal}(0, 14/6)\ [0.25, 14] \\ \mu_{\omega r} &\sim \text{Normal}(0, 30/6)\ [2, 30] \\ \mu_{\delta} &\sim \text{Normal}(20, 40/6)\ [0, 40]. \end{aligned} \tag{S11}$$

Note that we updated the prior means but kept the prior variances at their original wide values to avoid encoding over-confidence in the priors into the model. The posterior population means for these new sets of priors are depicted in **Figures S15-S16** (compare to **Figures S1-S2**). Overall, the findings were consistent across choices of prior.

	Alpha (%)	Delta (%)	Other VOI/VVOC (%)	Non-VOI/VOC (%)	Not genotyped (%)	Total (%)
Total	36 (20.8)	36 (20.8)	28 (16.2)	41 (23.7)	32 (18.5)	173 (100)
Age						
<18	3 (1.7)	2 (1.2)	2 (1.2)	0 (0)	1 (0.6)	8 (4.6)
18-29	23 (13.3)	6 (3.5)	13 (7.5)	26 (15)	11 (6.4)	79 (45.7)
30-39	4 (2.3)	8 (4.6)	6 (3.5)	7 (4.0)	6 (3.5)	31 (17.9)
40-49	4 (2.3)	14 (8.1)	4 (2.3)	3 (1.7)	5 (2.9)	30 (17.3)
50-59	2 (1.2)	4 (2.3)	1 (0.6)	2 (1.2)	4 (2.3)	13 (7.5)
≥60	0 (0)	2 (1.2)	2 (1.2)	3 (1.7)	5 (2.9)	12 (6.9)
Symptoms reported						
No	18 (10.4)	23 (13.3)	15 (8.7)	22 (12.7)	24 (13.9)	102 (59.0)
Yes	18 (10.4)	13 (7.5)	13 (7.5)	19 (11.0)	8 (4.6)	71 (41.0)
Vaccine breakthrough						
No	32 (18.5)	11 (6.4)	25 (14.5)	41 (23.7)	27 (15.6)	136 (78.6)
Yes	4 (2.3)	25 (14.5)	3 (1.7)	0 (0)	5 (2.9)	37 (21.4)

Table S1. Characteristics of the study population. Number and percent (in parentheses) of individuals in the study population by age group, reported symptoms, and vaccine breakthrough status, stratified by variant.

	Minimum Ct	Maximum viral concentration (log_{10} RNA copies/ml)	Proliferation duration (days)	Clearance duration (days)	Acute infection duration (days)
Non-VOI/VOC	20.1 [18.3, 21.7]	8.2 [7.7, 11.6]	4.2 [3.3, 5.2]	7.3 [6.1, 8.4]	11.4 [10.1, 12.8]
Alpha	21.0 [19.1, 20.9]	7.9 [8.0, 11.5]	3.4 [2.6, 4.5]	6.2 [5.2, 7.4]	9.6 [8.3, 11.1]
Delta	19.8 [18.0, 22.0]	8.3 [7.7, 11.6]	3.0 [2.2, 4.0]	6.2 [5.2, 7.4]	9.2 [8.0, 10.6]
Unvaccinated	20.7 [19.8, 20.2]	8.0 [8.2, 11.5]	3.5 [3.0, 4.0]	7.5 [6.8, 8.2]	11.0 [10.3, 11.8]
Vaccinated	20.5 [19.0, 21.0]	8.1 [7.9, 11.5]	3.2 [2.5, 4.0]	5.5 [4.6, 6.5]	8.7 [7.6, 9.9]

Table S2. Posterior population viral trajectory parameters for SARS-CoV-2 infections by variant and vaccination status. Reported values represent the posterior mean and 95% credible intervals (brackets) for each parameter.

Standard (copies/ul)	Replicate 1 (Ct)	Replicate 2 (Ct)	Average Ct
10^6	19.3	19.7	19.5
10^5	23.0	21.2	22.1
10^4	26.9	26.7	26.8
10^3	30.6	30.4	30.5
10^2	34.0	34.0	34.0
10^1	37.2	36.6	36.9
10^0	N/A	39.9	39.9

Table S3. Standard curve relationship between virus RNA copies and Ct values. Synthetic T7 RNA transcripts corresponding to a 1,363 base pair segment of the SARS-CoV-2 nucleocapsid gene were serially diluted from 10^6-10^0 and evaluated in duplicate with RT-qPCR. The best-fit linear regression of the average Ct on the log10-transformed standard values had slope -3.60971 and intercept 40.93733 (R^2 = 0.99).

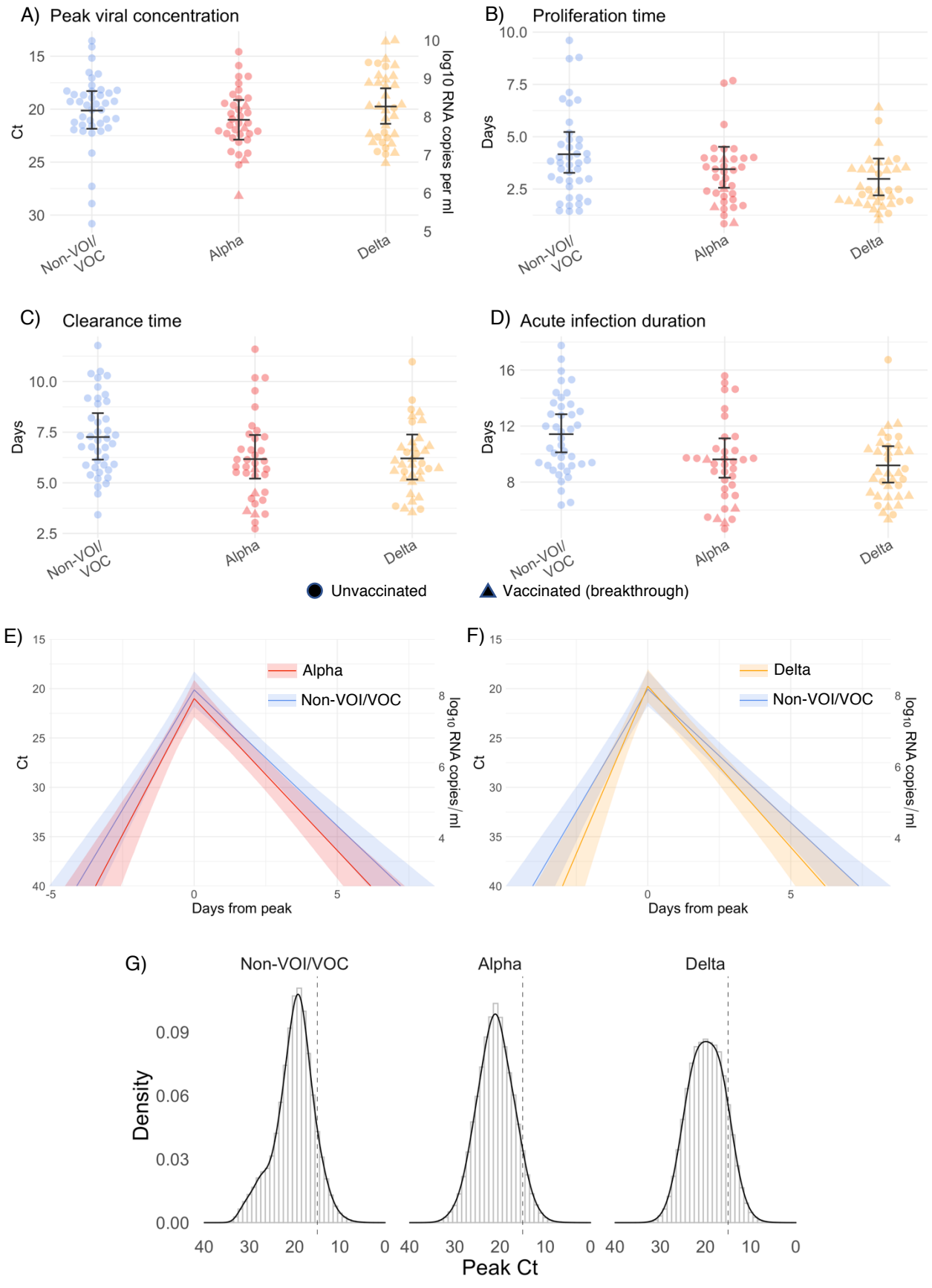
A) Peak viral concentration
Ct
log10 RNA copies per ml
Non-VOI/ VOC
Alpha
Delta
B) Proliferation time
Days
C) Clearance time
D) Acute infection duration
Unvaccinated
Vaccinated (breakthrough)
E)
Alpha
Non-VOI/VOC
log10 RNA copies/ml
Days from peak
F)
Delta
Non-VOI/VOC
G)
Density
Peak Ct

Figure S1. Estimated viral trajectory parameters for SARS-CoV-2 variants alpha and delta. Individual posterior means (points) with population means and 95% credible intervals (hatched lines) for (A) the peak viral concentration, (B) the proliferation duration, (C) the clearance duration, and (D) the total duration of acute infection for individuals infected with a non-VOI/VOC (light blue), alpha (red), or delta (orange). Circles denote unvaccinated individuals and triangles denote vaccinated individuals (breakthroughs). The points are jittered horizontally to avoid overlap. Panes (E)-(F) depict the mean posterior viral trajectories for alpha (E, red) and delta (F, orange) infections relative to non-VOI/VOC infections (light blue), as specified by the population means and credible intervals in (A)-(D). Solid lines in panes (E)-(F) depict the mean posterior viral trajectories and shaded regions represent 95% credible areas for the mean posterior trajectories. Histograms in pane (G) depict the posterior distributions of peak Ct values aggregated across all individuals infected with a non-VOI/VOC, alpha, and delta. The dashed line marks Ct = 15 (9.6 $\log_{10}$ RNA copies/ml) to facilitate comparison of the frequency of low peak Ct values/high peak viral concentrations across variants.

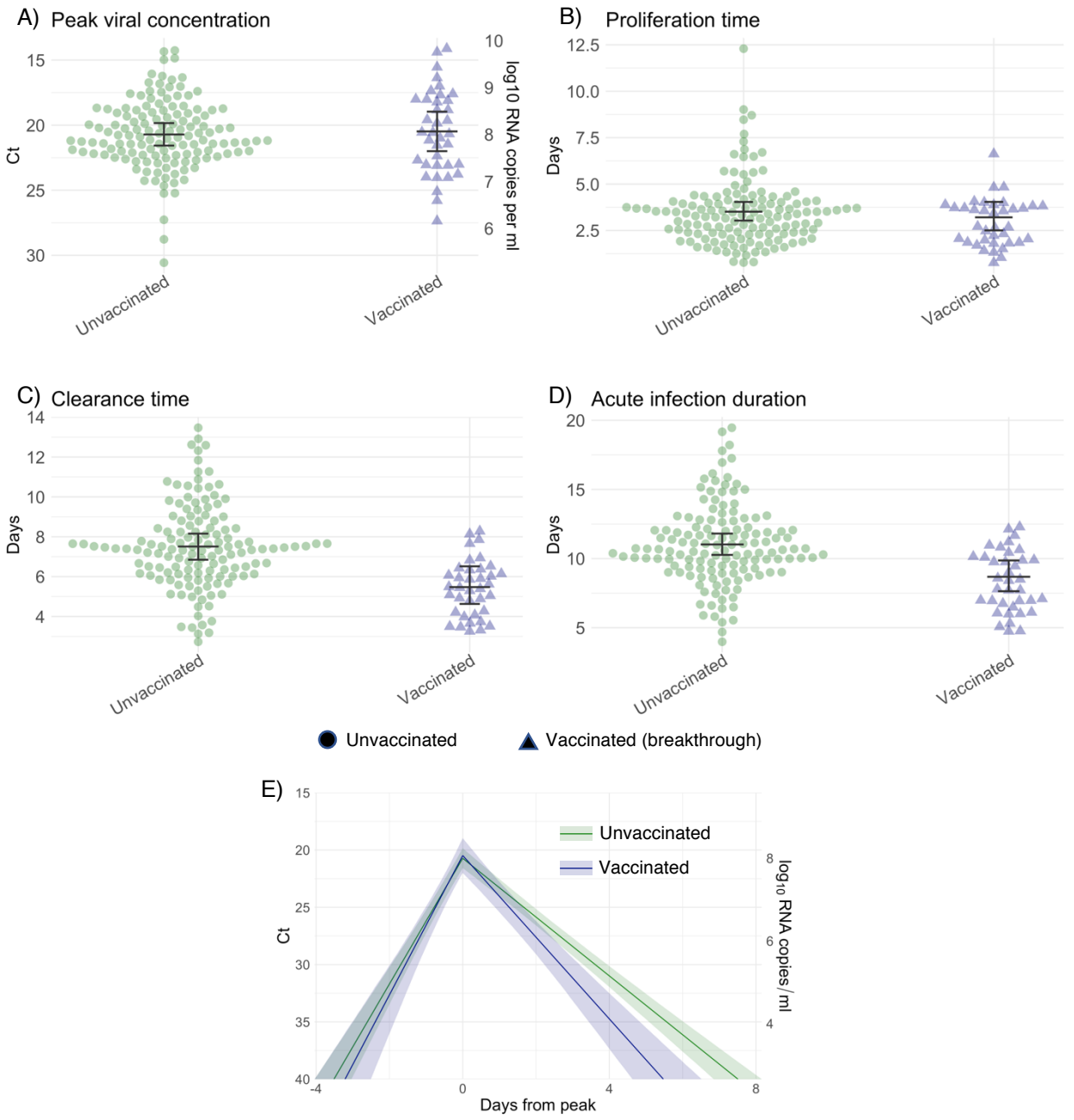

Figure S2. Estimated viral trajectory parameters for SARS-CoV-2 infections in unvaccinated and vaccinated individuals. Individual posterior means (points) with population means and 95% credible intervals (hatched lines) for (A) the peak viral concentration, (B) the proliferation duration, (C) the clearance duration, and (D) the total duration of acute infection for unvaccinated individuals (green) and vaccinated individuals (dark blue). Circles denote unvaccinated individuals and triangles denote vaccinated individuals (breakthroughs). The points are jittered horizontally to avoid overlap. Pane (E) depicts the mean posterior viral trajectories for vaccinated individuals (green) relative to unvaccinated individuals (dark blue), as specified by the population means and credible intervals in (A)-(D). Solid lines in pane (E) depict the mean posterior viral trajectories and shaded regions represent 95% credible areas for the mean posterior trajectories.

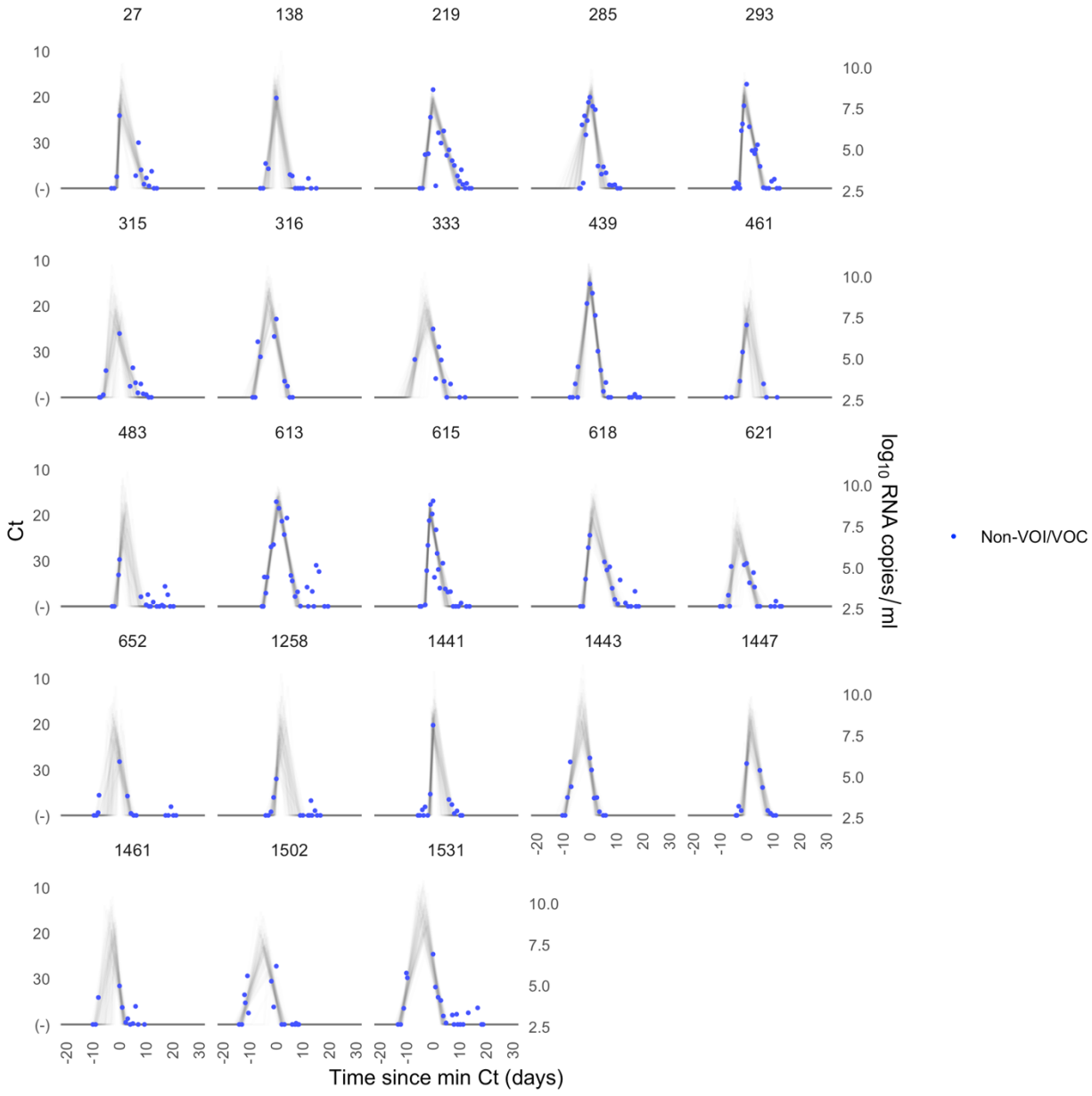

Figure S3. Ct values and estimated trajectories for non-VOI/VOC SARS-CoV-2 infections (1/2). Each pane depicts the recorded Ct values (points) and derived log-10 genome equivalents per ml (log(ge/ml)) for a single person during the study period. Points along the horizontal axis represent negative tests. Time is indexed in days since the minimum recorded Ct value (maximum viral concentration). Lines depict 100 draws from the posterior distribution for each person's viral trajectory. Shaded boxes denote breakthrough infections.

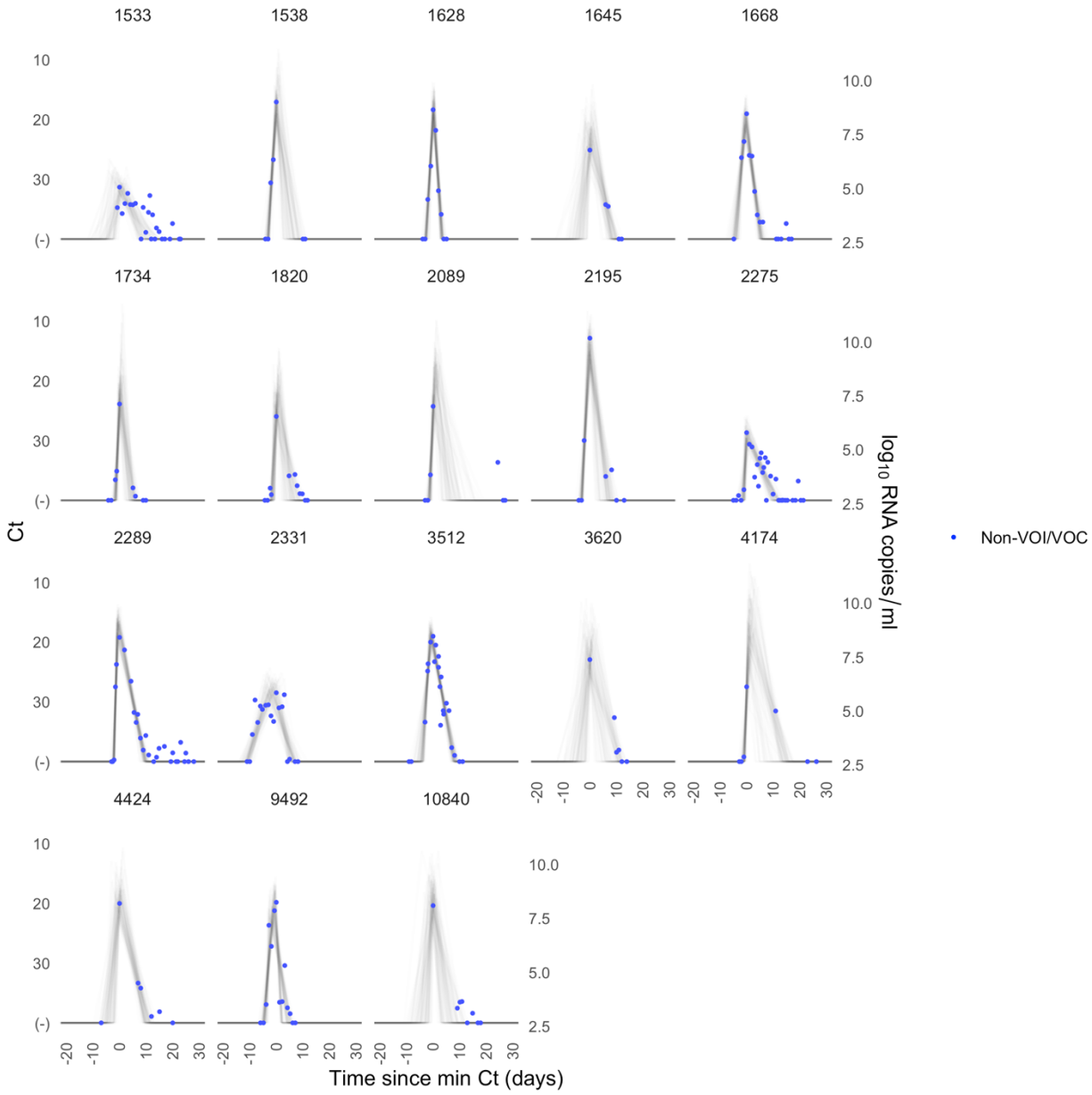

Figure S4. Ct values and estimated trajectories for non-VOI/VOC SARS-CoV-2 infections (2/2). Each pane depicts the recorded Ct values (points) and derived log-10 genome equivalents per ml (log(ge/ml)) for a single person during the study period. Points along the horizontal axis represent negative tests. Time is indexed in days since the minimum recorded Ct value (maximum viral concentration). Lines depict 100 draws from the posterior distribution for each person's viral trajectory. Shaded boxes denote breakthrough infections.

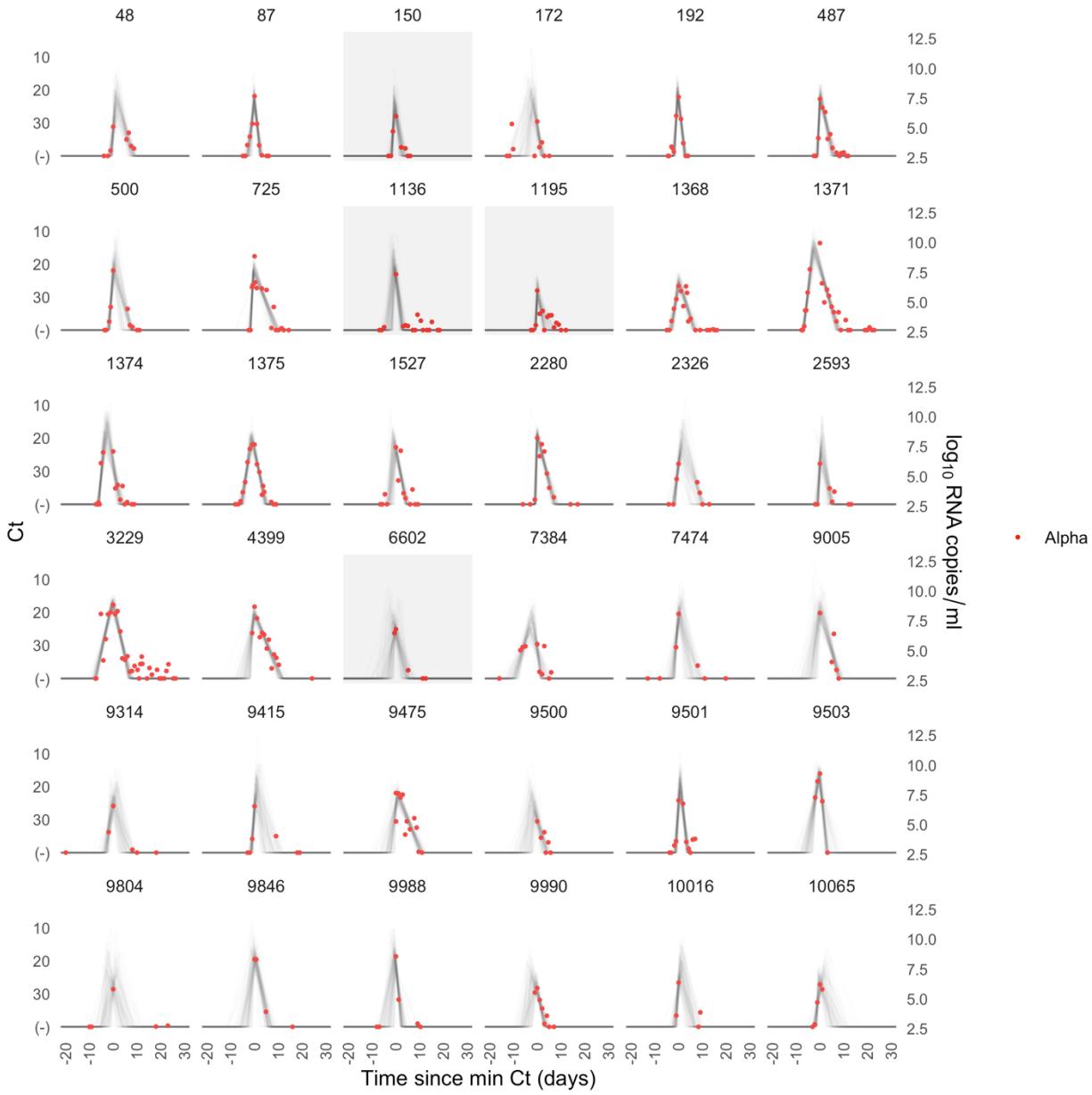

Figure S5. Ct values and estimated trajectories for alpha SARS-CoV-2 infections. Each pane depicts the recorded Ct values (points) and derived log-10 genome equivalents per ml (log(ge/ml)) for a single person during the study period. Points along the horizontal axis represent negative tests. Time is indexed in days since the minimum recorded Ct value (maximum viral concentration). Lines depict 100 draws from the posterior distribution for each person's viral trajectory. Shaded boxes denote breakthrough infections.

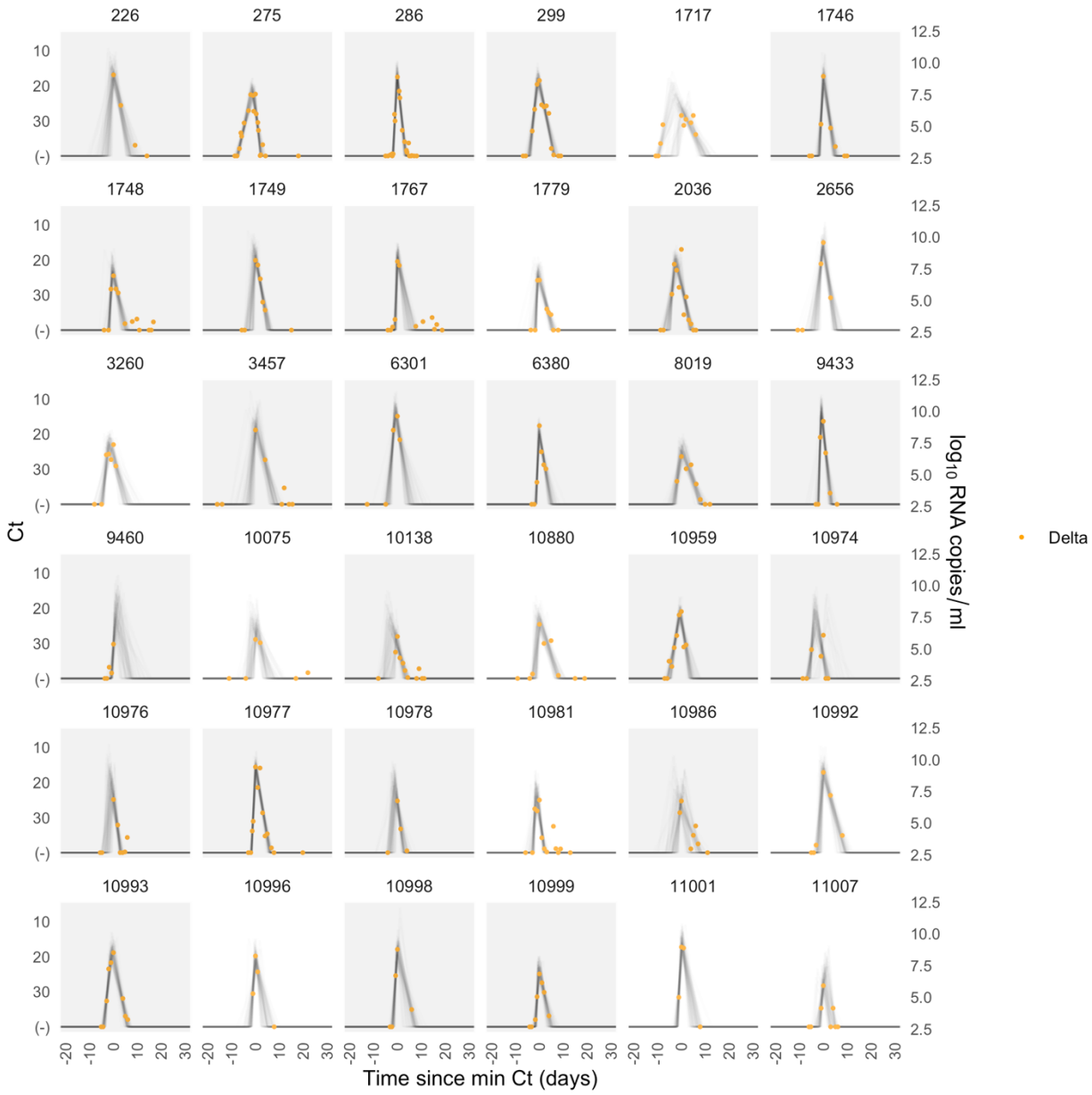

Figure S6. Ct values and estimated trajectories for delta SARS-CoV-2 infections. Each pane depicts the recorded Ct values (points) and derived log-10 genome equivalents per ml (log(ge/ml)) for a single person during the study period. Points along the horizontal axis represent negative tests. Time is indexed in days since the minimum recorded Ct value (maximum viral concentration). Lines depict 100 draws from the posterior distribution for each person's viral trajectory. Shaded boxes denote breakthrough infections.

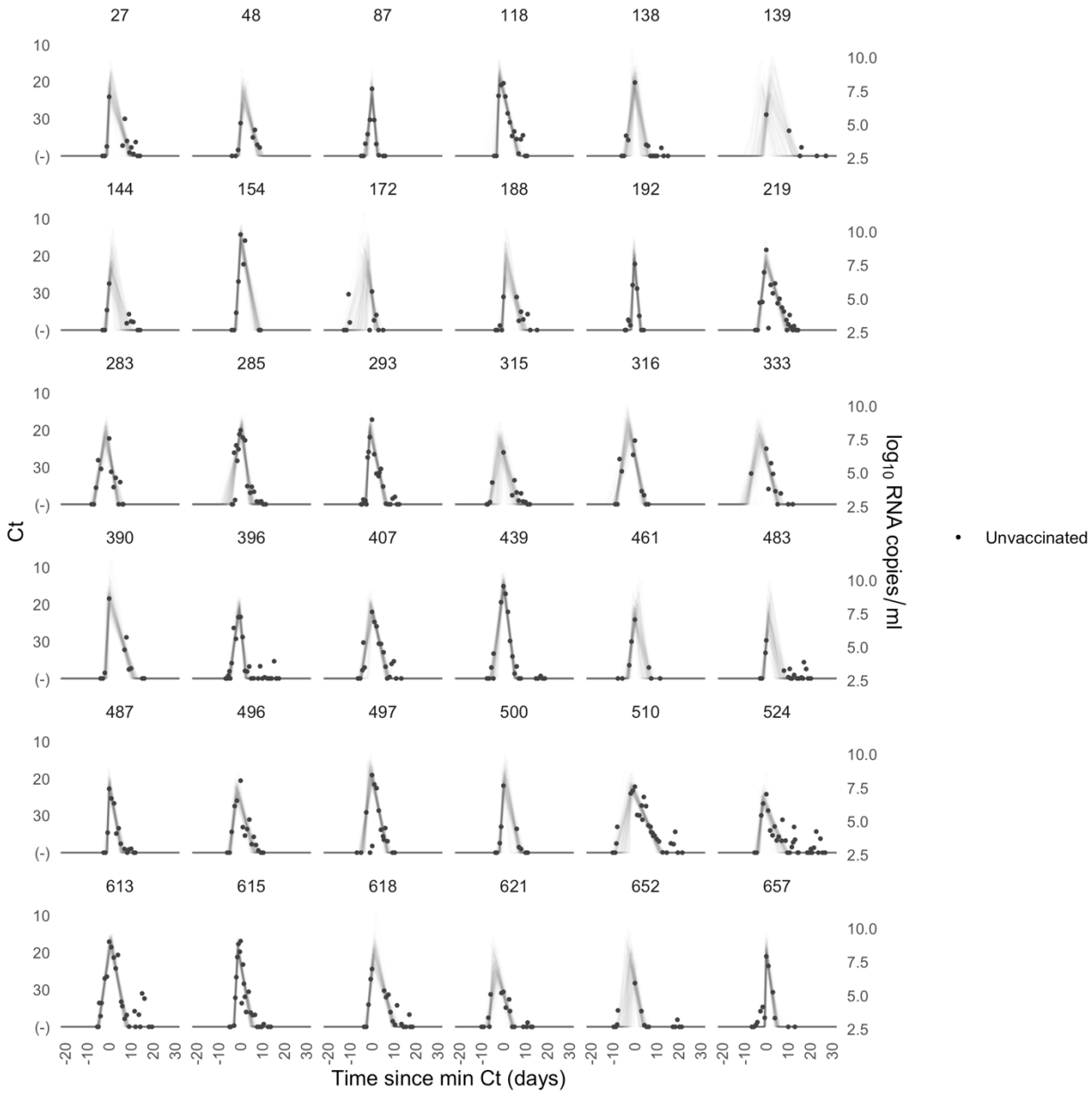

Figure S7. Ct values and estimated trajectories for SARS-CoV-2 infections in unvaccinated individuals (1/4). Each pane depicts the recorded Ct values (points) and derived log-10 genome equivalents per ml (log(ge/ml)) for a single person during the study period. Points along the horizontal axis represent negative tests. Time is indexed in days since the minimum recorded Ct value (maximum viral concentration). Lines depict 100 draws from the posterior distribution for each person's viral trajectory.

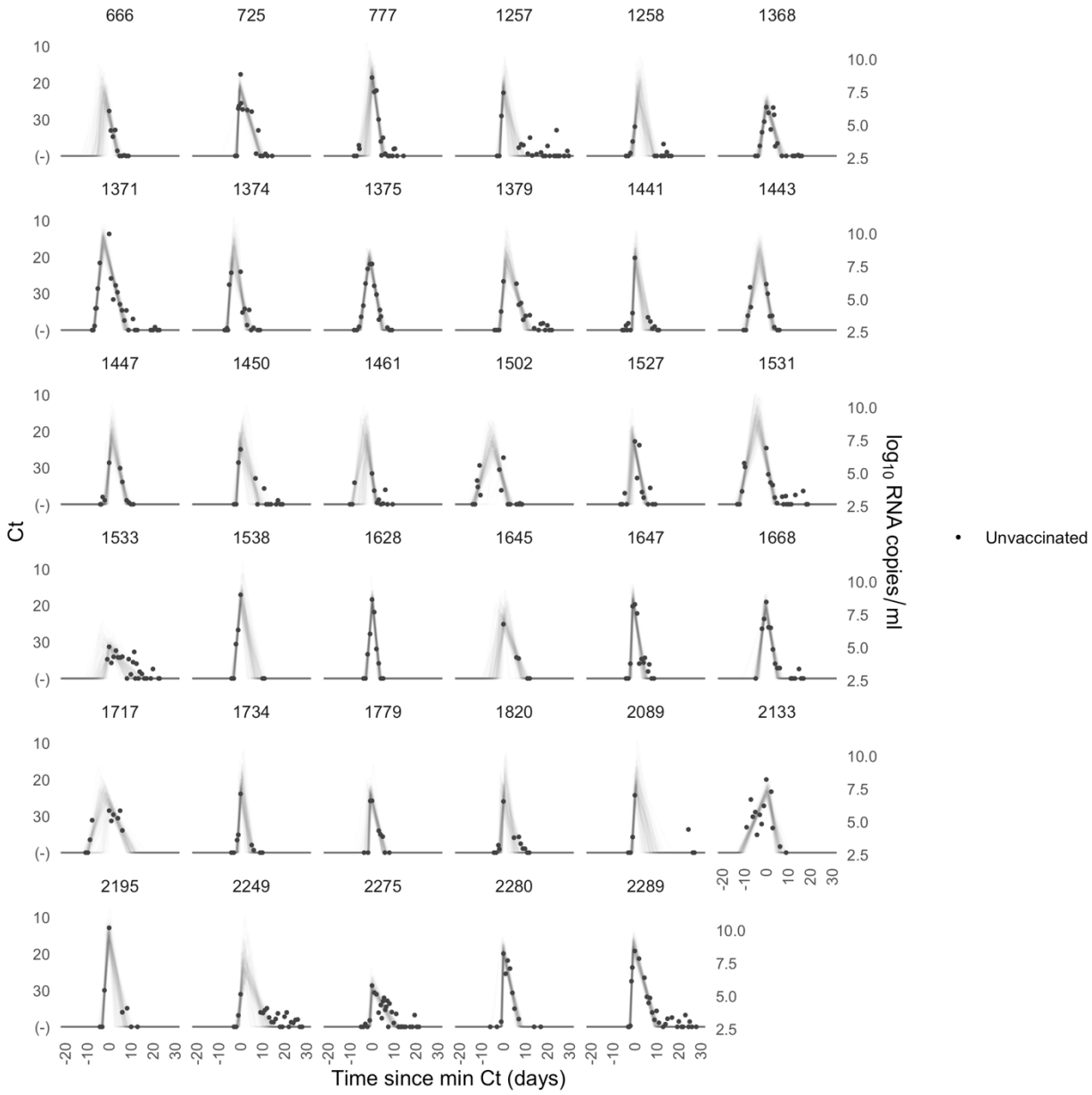

Figure S8. Ct values and estimated trajectories for SARS-CoV-2 infections in unvaccinated individuals (2/4). Each pane depicts the recorded Ct values (points) and derived log-10 genome equivalents per ml (log(ge/ml)) for a single person during the study period. Points along the horizontal axis represent negative tests. Time is indexed in days since the minimum recorded Ct value (maximum viral concentration). Lines depict 100 draws from the posterior distribution for each person's viral trajectory.

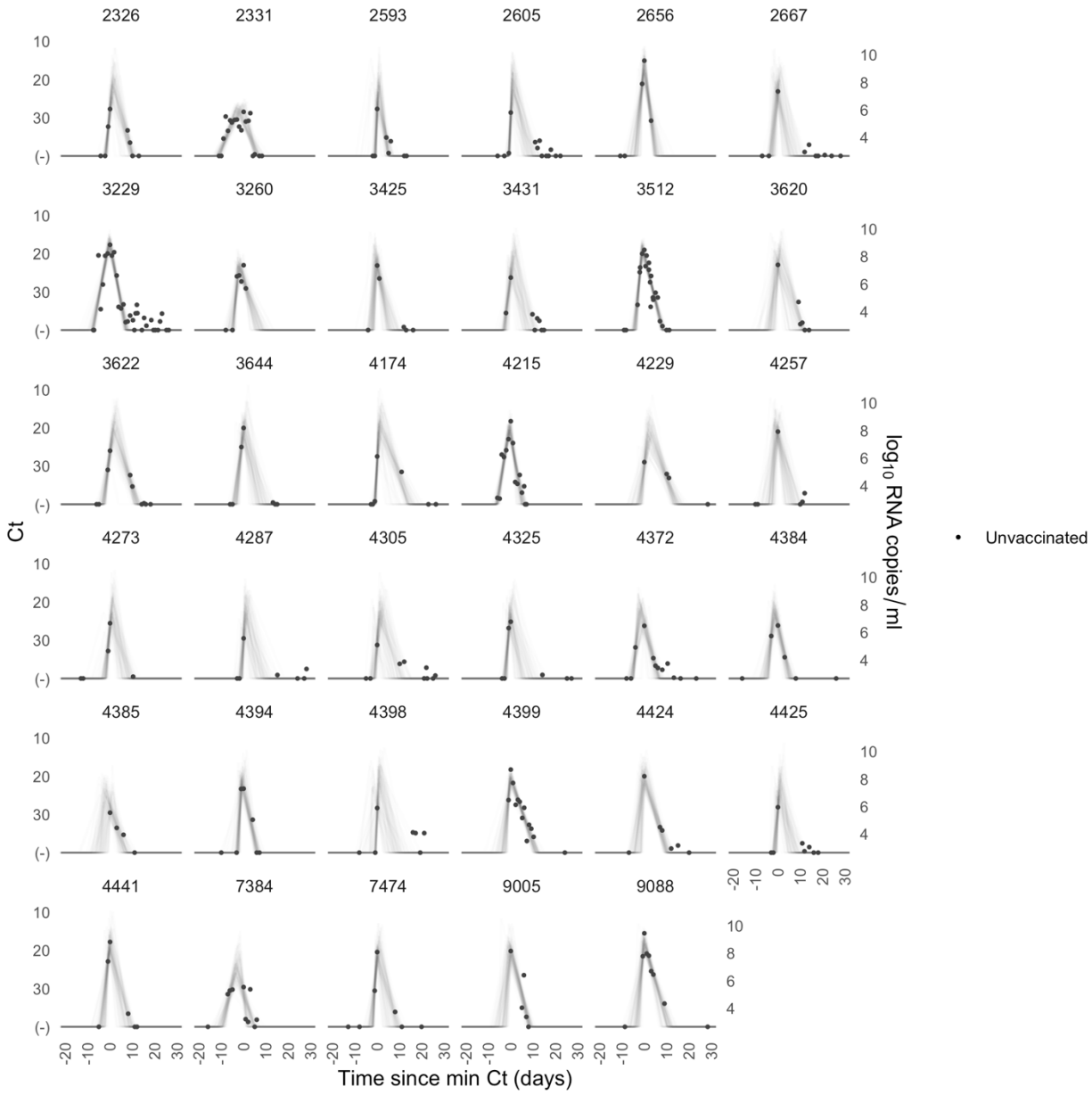

Figure S9. Ct values and estimated trajectories for SARS-CoV-2 infections in unvaccinated individuals (3/4). Each pane depicts the recorded Ct values (points) and derived log-10 genome equivalents per ml (log(ge/ml)) for a single person during the study period. Points along the horizontal axis represent negative tests. Time is indexed in days since the minimum recorded Ct value (maximum viral concentration). Lines depict 100 draws from the posterior distribution for each person's viral trajectory.

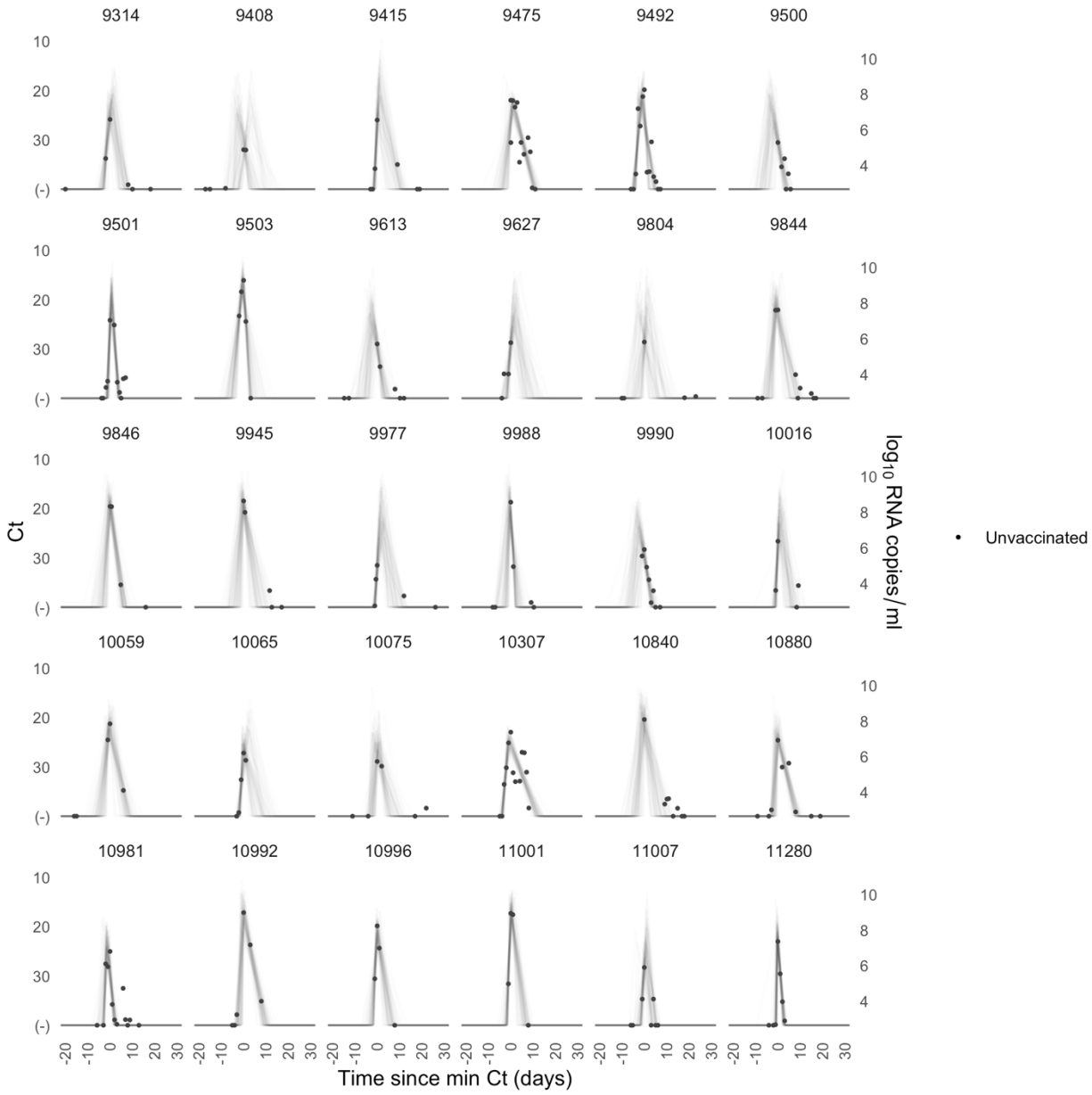

Figure S10. Ct values and estimated trajectories for SARS-CoV-2 infections in unvaccinated individuals (4/4). Each pane depicts the recorded Ct values (points) and derived log-10 genome equivalents per ml (log(ge/ml)) for a single person during the study period. Points along the horizontal axis represent negative tests. Time is indexed in days since the minimum recorded Ct value (maximum viral concentration). Lines depict 100 draws from the posterior distribution for each person's viral trajectory.

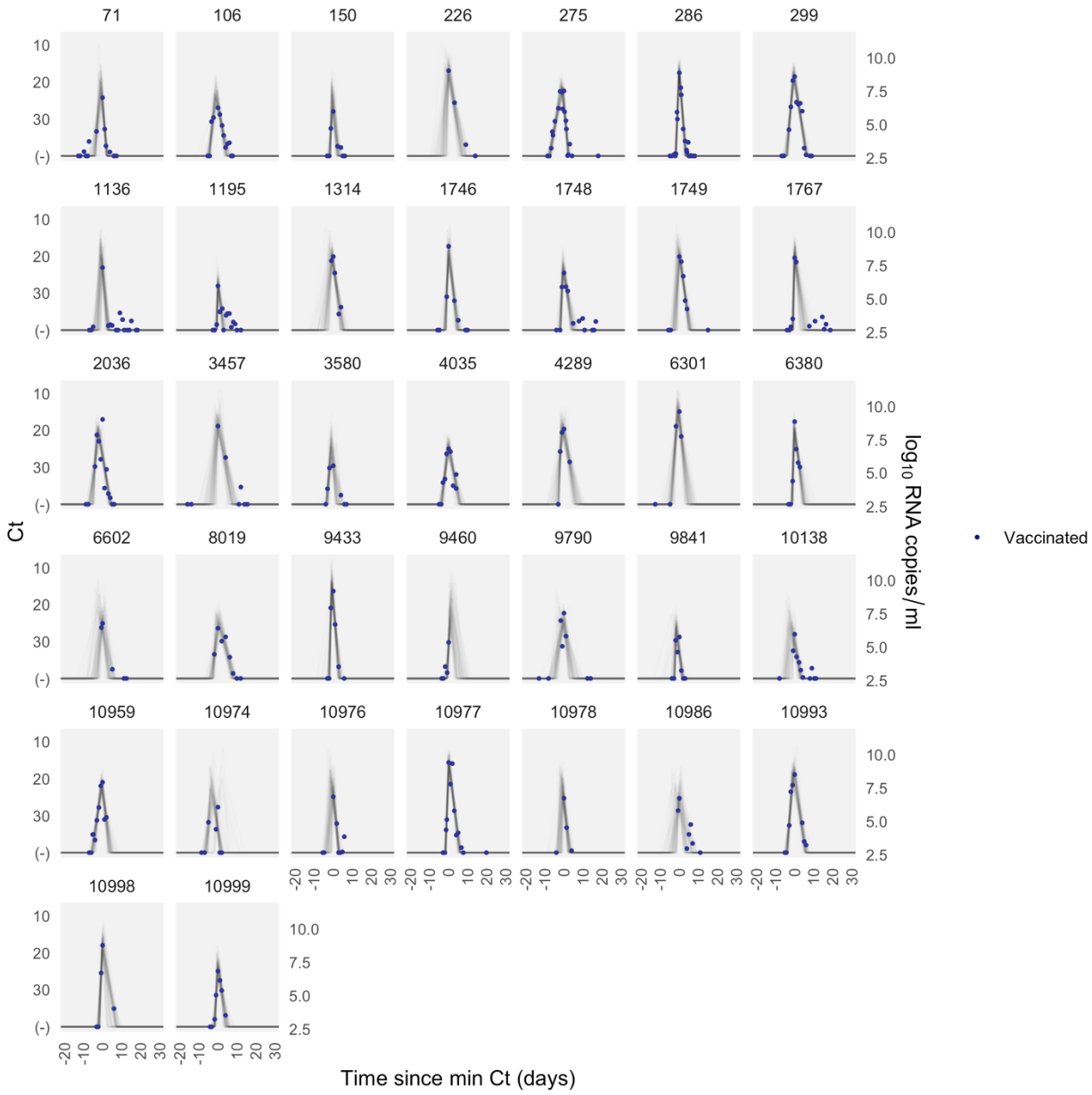

Figure S11. Ct values and estimated trajectories for SARS-CoV-2 infections in vaccinated individuals. Each pane depicts the recorded Ct values (points) and derived log-10 genome equivalents per ml (log(ge/ml)) for a single person during the study period. Points along the horizontal axis represent negative tests. Time is indexed in days since the minimum recorded Ct value (maximum viral concentration). Lines depict 100 draws from the posterior distribution for each person's viral trajectory. Shaded boxes denote breakthrough infections.

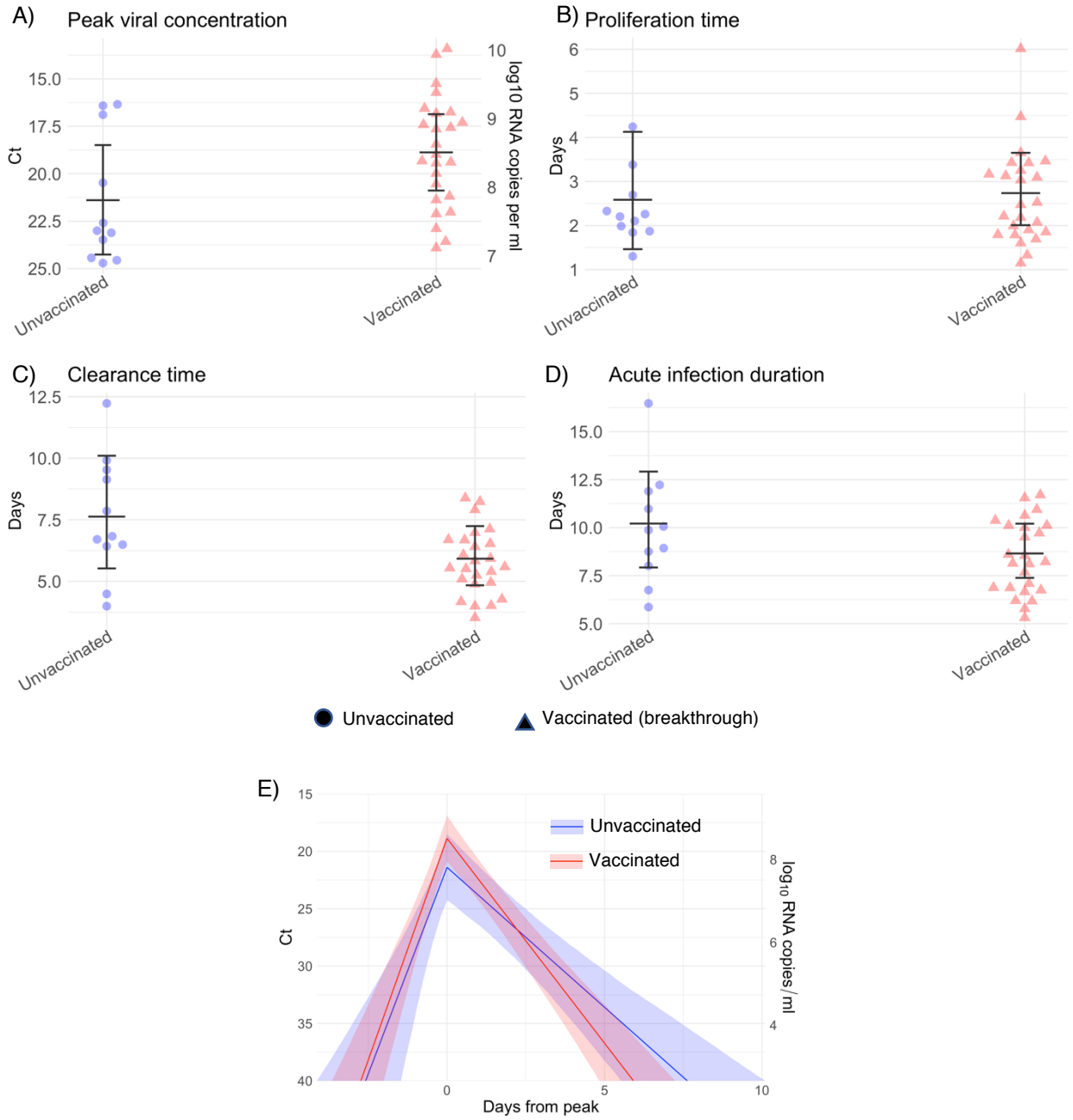

Figure S12. Estimated viral trajectory parameters for vaccinated and unvaccinated individuals infected with SARS-CoV-2 variant delta. Individual posterior means (points) with population means and 95% credible intervals (hatched lines) for (A) the peak viral concentration, (B) the proliferation duration, (C) the clearance duration, and (D) the total duration of acute infection for unvaccinated (blue) and vaccinated (red) individuals infected with delta. Circles denote unvaccinated individuals and triangles denote vaccinated individuals (breakthroughs). The points are jittered horizontally to avoid overlap. Pane (E) depicts the mean posterior viral trajectories for unvaccinated (blue) *vs.* vaccinated (red) individuals, as specified by the population means and credible intervals in (A)-(D). Solid lines in pane (E) depict the mean posterior viral trajectories and shaded regions represent 95% credible areas for the mean posterior trajectories.

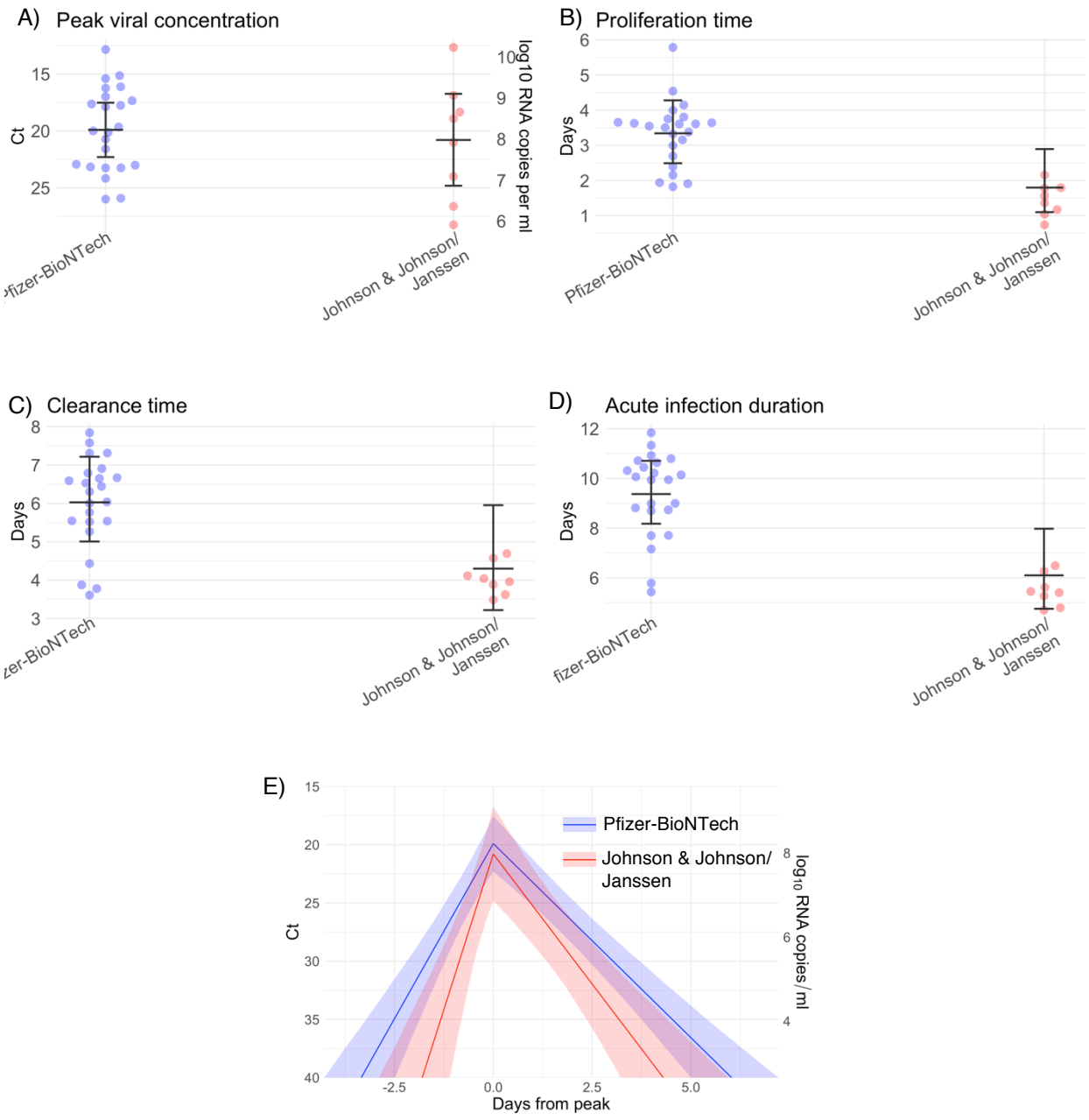

Figure S13. Estimated viral trajectory parameters for individuals vaccinated with the Pfizer-BioNTech vaccine vs. the Johnson & Johnson/Janssen vaccine. Individual posterior means (points) with population means and 95% credible intervals (hatched lines) for (A) the peak viral concentration, (B) the proliferation duration, (C) the clearance duration, and (D) the total duration of acute infection for breakthrough infections in individuals vaccinated with the Pfizer-BioNTech vaccine (blue) and the Johnson & Johnson/Janssen vaccine (red). The points are jittered horizontally to avoid overlap. Pane (E) depicts the mean posterior viral trajectories for breakthrough infections in individuals vaccinated with the Pfizer-BioNTech vaccine (blue) *vs.* the Johnson & Johnson/Janssen vaccine (red), as specified by the population means and credible intervals in (A)-(D). Solid lines in pane (E) depict the mean posterior viral trajectories and shaded regions represent 95% credible areas for the mean posterior trajectories.

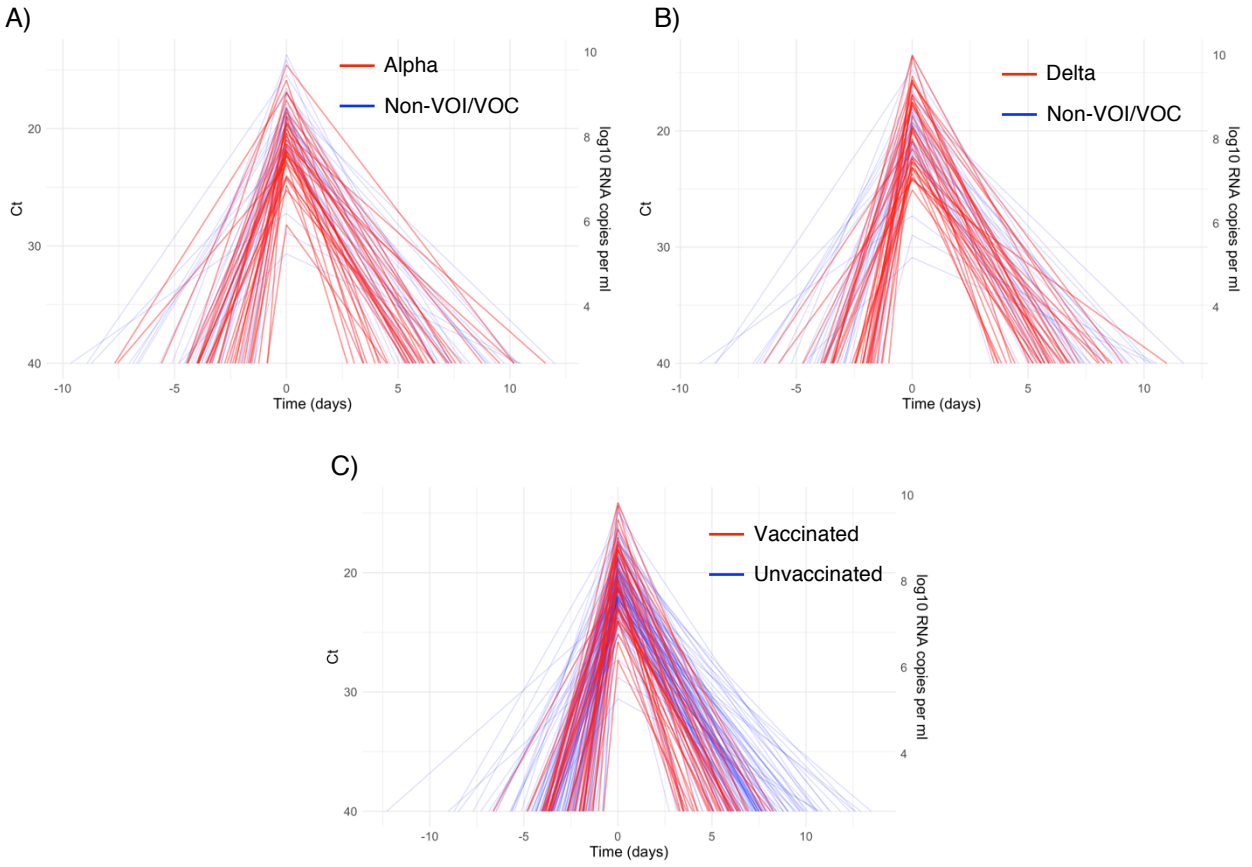

Figure S14. Mean posterior viral trajectories for each person. Pane (A) depicts alpha infections (red) against non-VOI/VOC infections (blue). Pane (B) depicts delta infections (red) against non-VOI/VOC infections (blue). Pane (C) depicts infections in vaccinated people (red) against unvaccinated people (blue). Trajectories are aligned temporally to have the same peak time.

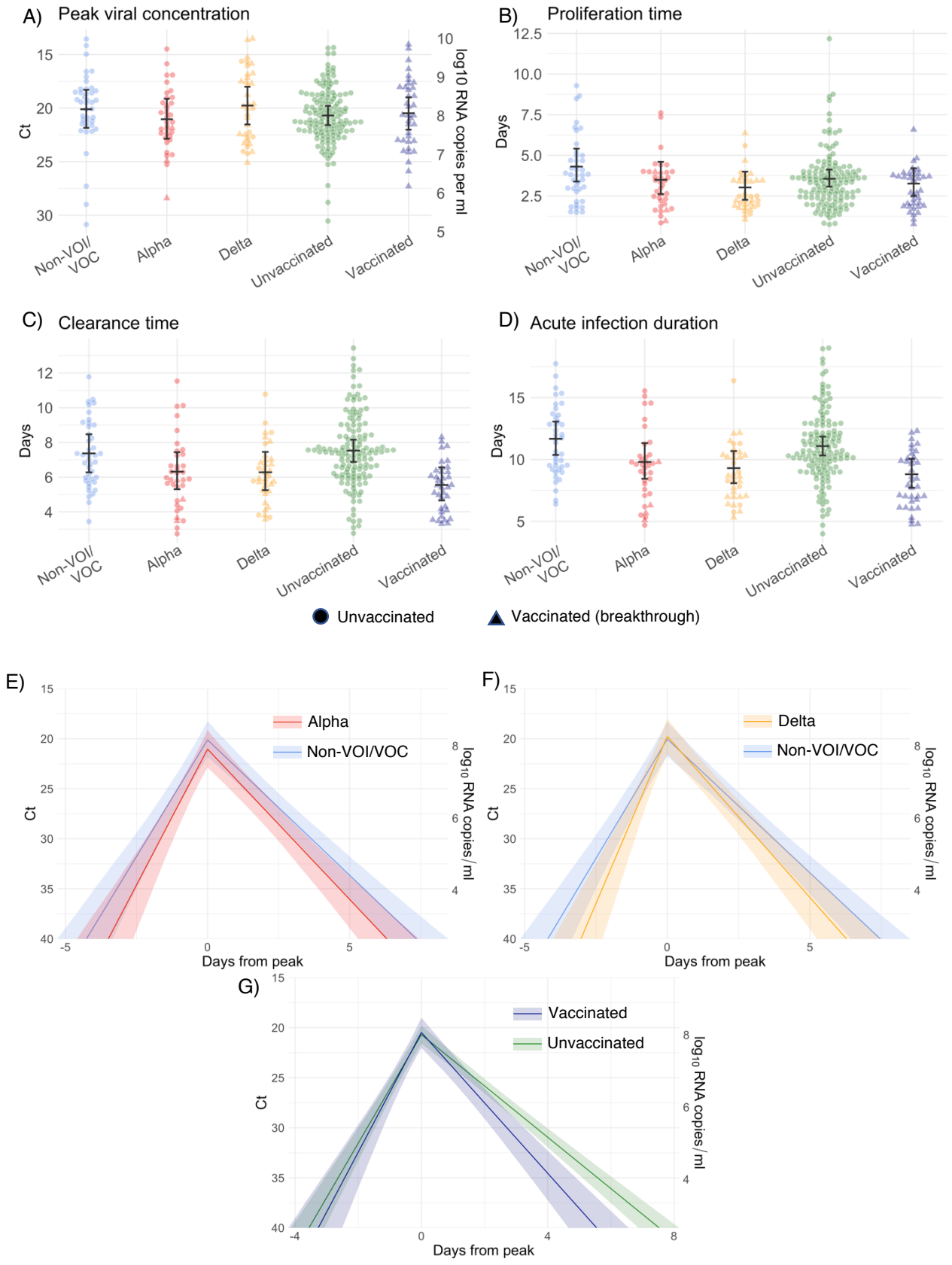
A) Peak viral concentration
Ct
log10 RNA copies per ml
Non-VOI/ VOC
Alpha
Delta
Unvaccinated
Vaccinated
B) Proliferation time
Days
C) Clearance time
D) Acute infection duration
Unvaccinated
Vaccinated (breakthrough)
E)
Alpha
Non-VOI/VOC
log10 RNA copies/ml
Days from peak
F)
Delta
Non-VOI/VOC
G)
Vaccinated
Unvaccinated

Figure S15. Estimated viral trajectory parameters for SARS-CoV-2 infections by variant and vaccination status using uninformative priors. Individual posterior means (points) with population means and 95% credible intervals (hatched lines) for (A) the peak viral concentration, (B) the proliferation duration, (C) the clearance duration, and (D) the total duration of acute infection for individuals infected with a non-VOI/VOC (blue), alpha (red), or delta (purple), and for individuals who were unvaccinated (green) or vaccinated (maroon). Circles denote unvaccinated individuals and triangles denote vaccinated individuals (breakthroughs). The points are jittered horizontally to avoid overlap. Solid lines in panes (E)-(F) depict the mean posterior viral trajectories for alpha (E, red) and delta (F, purple) infections respectively relative to non-VOI/VOC infections (blue), as specified by the population means and credible intervals in (A)-(D). Solid lines in pane (G) depict the mean posterior viral trajectory for vaccinated (maroon) relative to unvaccinated (green) individuals. The shaded regions in (E)-(G) represent 95% credible areas for the mean population trajectories. Priors were chosen to be uninformative and are defined in Eq. (S10).

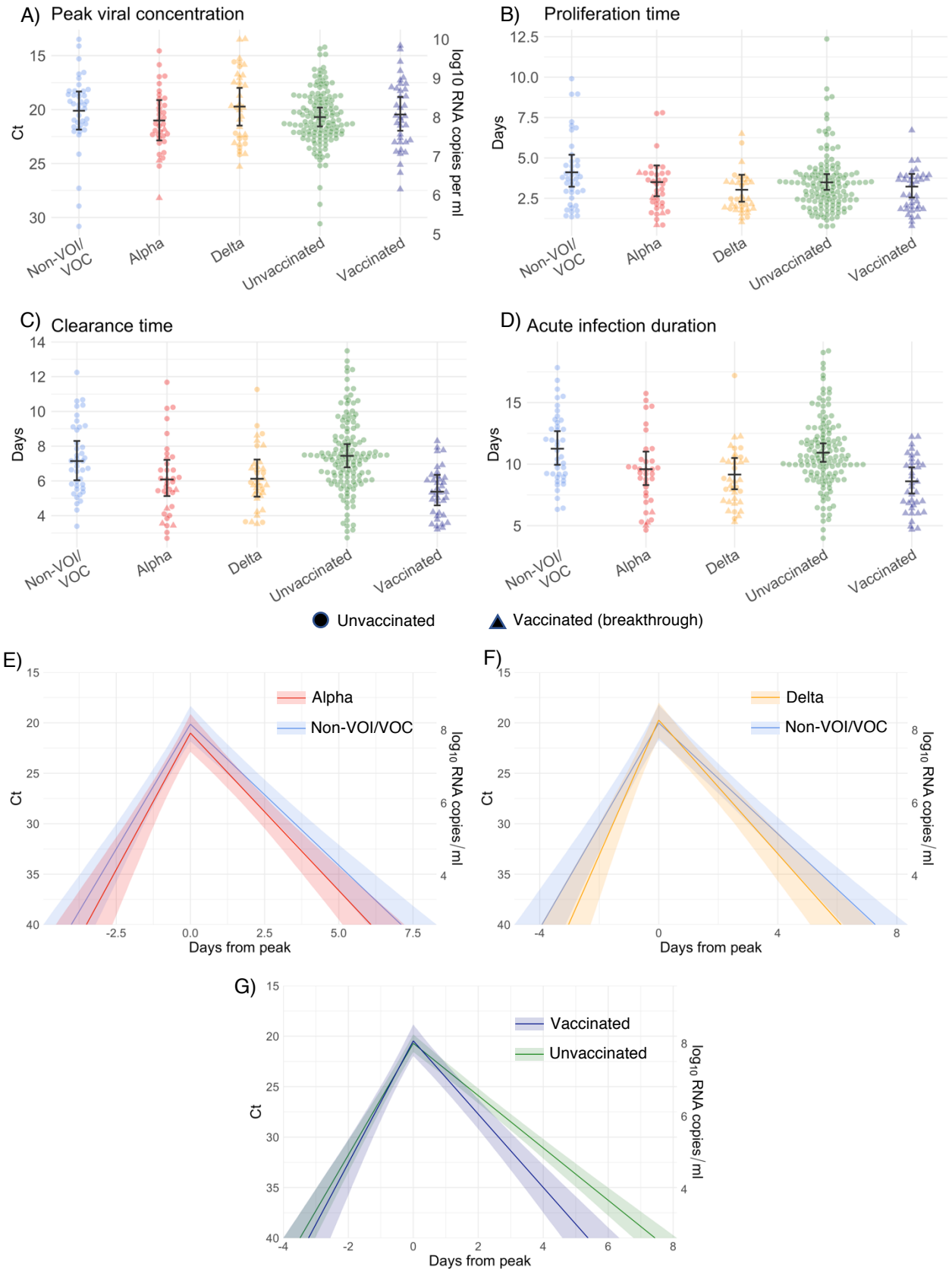
A) Peak viral concentration
Ct
log10 RNA copies per ml
Non-VOI/ VOC
Alpha
Delta
Unvaccinated
Vaccinated
B) Proliferation time
Days
C) Clearance time
D) Acute infection duration
Unvaccinated
Vaccinated (breakthrough)
E)
Alpha
Non-VOI/VOC
log10 RNA copies/ml
Days from peak
F)
Delta
Non-VOI/VOC
G)
Vaccinated
Unvaccinated

Figure S16. Estimated viral trajectory parameters for SARS-CoV-2 infections by variant and vaccination status using biased (low) priors. Individual posterior means (points) with population means and 95% credible intervals (hatched lines) for (A) the peak viral concentration, (B) the proliferation duration, (C) the clearance duration, and (D) the total duration of acute infection for individuals infected with a non-VOI/VOC (blue), alpha (red), or delta (purple), and for individuals who were unvaccinated (green) or vaccinated (maroon). Circles denote unvaccinated individuals and triangles denote vaccinated individuals (breakthroughs). The points are jittered horizontally to avoid overlap. Solid lines in panes (E)-(F) depict the mean posterior viral trajectories for alpha (E, red) and delta (F, purple) infections respectively relative to non-VOI/VOC infections (blue), as specified by the population means and credible intervals in (A)-(D). Solid lines in pane (G) depict the mean posterior viral trajectory for vaccinated (maroon) relative to unvaccinated (green) individuals. The shaded regions in (E)-(G) represent 95% credible areas for the mean population trajectories. Priors were chosen to be unrealistically low and are defined in Eq. (S11).

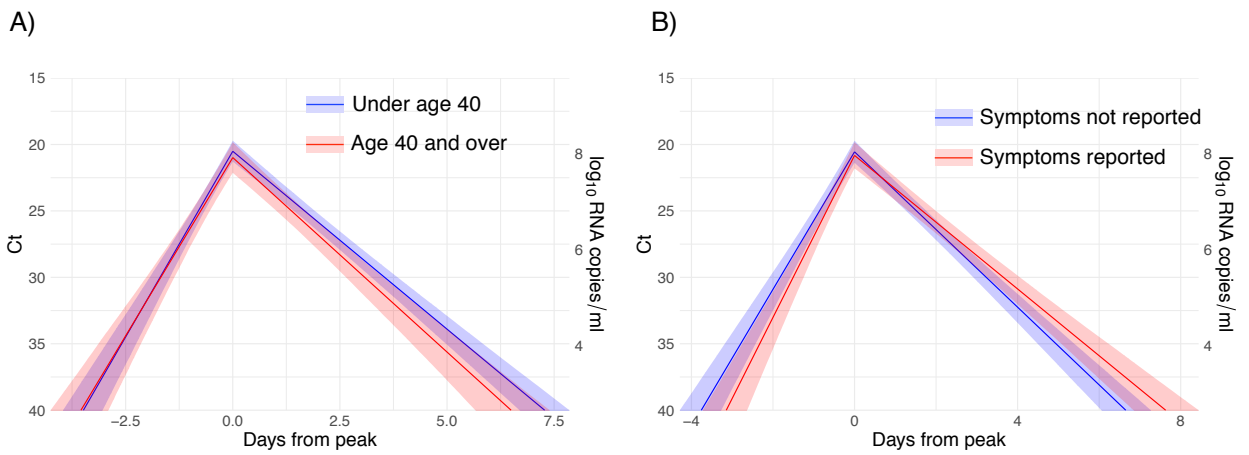

Figure S17. Posterior viral trajectory inferences for (A) individuals over age 40 (red) *vs.* everyone else (blue), and (B) individuals who reported symptoms (red) *vs.* everyone else (blue). Solid lines depict the mean posterior viral trajectories. Shaded regions represent 95% credible areas for the mean population trajectories. Priors were chosen to be uninformative and are defined in Eq. (S10).

References.

1. United States Food and Drug Administration. *Emergency Use Authorization for TaqPath COVID-19 Combo Kit*.; 2020. https://www.fda.gov/media/136113/download
2. Loman N, Rowe W, Rambaut A. nCoV-2019 novel coronavirus bioinformatics protocol.
3. Illumina. *Illumina COVIDSeq Test Instructions for Use*.; 2021. https://www.fda.gov/media/138776/download
4. Illumina. NextSeq 550 System Documentation. Published 2021. Accessed June 10, 2021. https://support.illumina.com/sequencing/sequencing_instruments/nextseq-550/documentation.html
5. BaseSpace Labs. DRAGEN COVID Lineage. Published online 2021.
6. Rambaut A, Holmes EC, O'Toole Á, Hill V, McCrone JT, Ruis C, et al. A dynamic nomenclature proposal for SARS-CoV-2 lineages to assist genomic epidemiology. *Nat Microbiol*. 2020;5(11):1403-1407. doi:10.1038/s41564-020-0770-5
7. Aksamentov I, Neher R. NextClade. Published 2021. Accessed June 10, 2021. https://clades.nextstrain.org/
8. Kudo E, Israelow B, Vogels CBF, Lu P, Wyllie AL, Tokuyama M, et al. Detection of SARS-CoV-2 RNA by multiplex RT-qPCR. Sugden B, ed. *PLOS Biol*. 2020;18(10):e3000867. doi:10.1371/journal.pbio.3000867
9. Kissler SM, Fauver JR, Mack C, Olesen SW, Tai C, Shiue KY, et al. Viral dynamics of acute SARS-CoV-2 infection and applications to diagnostic and public health strategies. *PLoS Biol*. 2021;19(7):1-17. doi:10.1371/journal.pbio.3001333
10. Vogels C, Fauver J, Ott IM, Grubaugh N. *Generation of SARS-COV-2 RNA Transcript Standards for QRT-PCR Detection Assays*.; 2020. doi:10.17504/protocols.io.bdv6i69e
11. Carpenter B, Gelman A, Hoffman MD, Lee D, Goodrich B, Betancourt M, et al. Stan : A Probabilistic Programming Language. *J Stat Softw*. 2017;76(1). doi:10.18637/jss.v076.i01
12. Kissler SM. Github Repository: CtTrajectories_AllVariants. Published 2021. Accessed June 14, 2021. https://github.com/gradlab/CtTrajectories_AllVariants
13. Cleary B, Hay JA, Blumenstiel B, Gabriel S, Regev A, Mina MJ. Efficient prevalence estimation and infected sample identification with group testing for SARS-CoV-2. *medRxiv*. Published online 2020.
14. Tom MR, Mina MJ. To Interpret the SARS-CoV-2 Test, Consider the Cycle Threshold Value. *Clin Infect Dis*. 2020;02115(Xx):1-3. doi:10.1093/cid/ciaa619
15. R Development Core Team R. R: A Language and Environment for Statistical Computing. Team RDC, ed. *R Found Stat Comput*. 2011;1(2.11.1):409. doi:10.1007/978-3-540-74686-7
16. Kissler SM, Fauver JR, Mack C, Olesen SW, Tai C, Shiue KY, et al. Viral dynamics of acute SARS-CoV-2 infection and applications to diagnostic and public health strategies. Riley S, ed. *PLOS Biol*. 2021;19(7):e3001333. doi:10.1371/journal.pbio.3001333